Published in final edited form as:
J Proteome Res. 2010 July 2; 9(7): 3656–3663. doi:10.1021/pr100164x.

Proteomic Analysis of Laser Microdissected Melanoma Cells from Skin Organ Cultures

Brian L. Hood[1,3,#], **Jelena Grahovac**[2,#], **Melanie S. Flint**[1,3], **Mai Sun**[1,3], **Nuno Charro**[3], **Dorothea Becker**[2], **Alan Wells**[2,4,*], and **Thomas P Conrads**[1,2,*]

[1]Department of Pharmacology & Chemical Biology, University of Pittsburgh Cancer Institute, University of Pittsburgh

[2]Department of Pathology, University of Pittsburgh Cancer Institute, University of Pittsburgh

[3]Department of Mass Spectrometry Platform, Cancer Biomarkers Facility, University of Pittsburgh Cancer Institute, University of Pittsburgh

[4]Pittsburgh VA HealthCare System

Abstract

Gaining insights into the molecular events that govern the progression from melanoma *in situ* to advanced melanoma, and understanding how the local microenvironment at the melanoma site influences this progression, are two clinically pivotal aspects that to date are largely unexplored. In an effort to identify key regulators of the crosstalk between melanoma cells and the melanoma-skin microenvironment, primary and metastatic human melanoma cells were seeded into skin organ cultures (SOCs), and grown for two weeks. Melanoma cells were recovered from SOCs by laser microdissection and whole-cell tryptic digests analyzed by nanoflow liquid chromatography-tandem mass spectrometry with an LTQ-Orbitrap. The differential protein abundances were calculated by spectral counting, the results of which provides evidence that cell-matrix and cell-adhesion molecules that are upregulated in the presence of these melanoma cells recapitulate proteomic data obtained from comparative analysis of human biopsies of invasive melanoma and a tissue sample of adjacent, non-involved skin. This concordance demonstrates the value of SOCs for conducting proteomic investigations of the melanoma microenvironment.

Keywords

melanoma; proteomics; skin organ culture

Introduction

Despite increasing efforts aimed at melanoma prevention and, equally important, early detection, the worldwide incidence of melanoma continues to rise. As there are no effective treatment regimens for patients with advanced melanoma, the molecular basis of melanoma progression is likely to hold the key to clinical treatment. Melanoma progression is a

[*]**Corresponding authors:** Thomas P. Conrads, Ph.D., 204 Craft Avenue, Suite B401, Pittsburgh, PA, 15213, Tel: 412-641-7556, Fax: 412-641-2356, conradstp@upmc.edu, and Alan Wells, M.D., S713 Scaife Hall, 3550 Terrace Street, Pittsburgh, PA 15213, Tel: 412-647-7813, Fax: 412-647-8567, wellsa@upmc.edu.
[#]These authors contributed equally to this work.

Supplemental Information
The complete list of peptides/proteins, identified in the various SOC sections and the melanoma and skin tissue samples are listed in Supplemental Table S1 which can be accessed at http://pubs.acs.org.

pathologically well-defined process and when surgically resected with a wide and deep margin, the prognosis for patients with melanoma *in situ* is favorable. While melanoma *in situ* is confined to the epidermis, primary melanoma in the vertical growth phase (VGP) has invaded deep into the dermis and, unlike melanoma *in situ* but like melanoma in the metastatic growth phase (MGP), VGP melanoma proliferates aggressively.

Over the past few years, high-throughput studies such as serial analysis of gene expression (SAGE), whole-genome microarray expression profiling and integrative analysis by microarray-based comparative genomic hybridization (array-CGH) have led to the identification of genes that previously were not known to be expressed in advanced melanomas, and/or were found to be upregulated with progression from early to advanced-stage melanoma. More recently, mass spectrometry (MS)-based proteomics has been used to identify proteins that are differentially expressed in VGP versus MGP melanomas1, or to detect melanoma in its early stage of development2–4. Unlike in the case of breast cancer, however, where various high-throughput molecular approaches have generated significant information detailing the interactions among epithelial and stromal cells that play supporting roles in tumorigenesis5, little information is yet available regarding the contributions of the local microenvironment to melanoma invasion and progression.

The epidermis is a multilayered structure, which is separated by an intact basement membrane from mesenchymal support cells. The stem cell-like basal keratinocytes undergo asymmetric replications with a multi-cell vertical differentiation resulting in enucleation and formation of a keratinized barrier. Neuroectoderm-derived melanocytes migrate into and reside in the epidermis where they are in contact with and communicate through E-cadherin and connexin junctions with keratinocytes. As part of the invasion process, melanoma cells must transit an E-cadherin-bridged epithelial milieu, attach to and breach the laminin/fibronectin-rich basement membrane and penetrate the dermis to reach conduits for dissemination, such as the host vasculature (Fig. 1A). Detailed insights are lacking regarding how the local microenvironment affects or alters molecular features of melanoma cells that may be required to drive invasion and progression, arising from the absence of suitable skin models that mimic invasive growth. Indeed, rodent skin does not recapitulate the structural microenvironment of human skin and other animal models, such as porcine, do not present naturally occurring melanomas. *Ex vivo* human skin organ cultures (SOCs; Fig. 1B) have been used to investigate various human skin conditions including wound healing and have been used in a limited fashion in melanoma research6–10. Skin organ cultures are derived from excess pathological specimens obtained during cosmetic surgery or post bariatric weight loss, or can be generated *ex vivo* from human skin components11.

In the present study, we demonstrate that seeding VGP and MGP melanoma cells into SOCs leads to formation of melanoma nodules after approximately 12 days. Laser microdissection was utilized to acquire the melanoma tumor nodule from these tissue sections, as well as samples from collagen-injected and non-injected SOCs, which were analyzed by nanoflow liquid chromatography-tandem mass spectrometry (LC-MS/MS). An analysis of differential protein abundances by spectral counting was conducted, and demonstrates that the proteomic profiles very closely resemble that obtained from a differential proteomic analysis of human melanoma and an adjacent skin biopsy free of melanoma. These data suggest that melanoma-seeded SOCs represent a unique model system for investigating the molecular events in the microenvironment that promote melanoma invasion and progression.

Materials and Methods

Cell Cultures and Tissue Samples

Normal human epidermal melanocytes (FC-0019, Lifeline Cell Technology, Walkersville, MD) were maintained in DermaLife Basal Medium with LifeFactors (LM-0027, Lifeline Cell Technology). The VGP (WM983-A) and MGP (WM1158) human melanoma cell lines were propagated *in vitro* as described12. Deidentified, post-diagnosis, excess pathological specimens, representing an advanced melanoma and an adjacent skin biopsy with no clinical signs of melanoma, resected from a patient, were obtained in compliance with a University of Pittsburgh Cancer Institute (UPCI) and University of Pittsburgh Institutional Review Board (IRB)-approved protocol.

Antibodies and Reagents

An anti-human/mouse Tenascin-C monoclonal antibody (MAB2138) was purchased from R&D Systems (Minneapolis, MN), and mouse anti-α-actinin-4 antibody (sc-49333) was from Santa Cruz Biotechnology, Inc. (Santa Cruz, CA). Antibodies were used at a 1:200 dilution for immunoblotting and immunocytochemistry. For immunohistochemistry stainings, anti-human tensacin-C mouse monoclonal antibody (ab6393) and anti-human/mouse α-actinin 4 antibody (ab32816, Abcam, Cambridge, MA) were used at the final concentration of 2 μg/ml.

Skin Organ Cultures

Skin organ culture experiments were performed on human Epiderm full-thickness 400 (EFT-400) 3D skin-like structures obtained from MatTek Corporation (Ashland, MA). These constructs contain human-derived dermal fibroblasts and epidermal keratinocytes and utilize bovine collagen as the base for the dermal matrix. Cultures were maintained at the air-liquid interface and supplied every other day with maintenance medium (EFT-400-MM, MatTek). Cultures were injected intra-epidermaly with 10,000 melanoma cells (either WM983-A or WM1158) resuspended in 3 μg/mL rat tail collagen (R&D Systems). Collagen-injection and non-injected SOCs served as controls. On day 13 after injection, tissues were divided in half with a razor; one half was formalin-fixed and paraffin-embedded, and the other half was embedded in OCT and frozen in liquid nitrogen. This time point was chosen based on previous reports as sufficient time for growth of tumor-like structures within the SOC.6, 8 Furthermore, the SOC maintain structural integrity for throughout this time period but begin to degenerate upon further culture. Cells from defined regions were acquired by laser microdissection (Leica LMD 6000, Leica Microsystems, Inc., Bannockburn, IL) and collected in 40 μL of purified H_2O in RNAase/DNAse-free microcentrifuge tubes.

FFPE Sample Preparation

Samples were brought to 100 mM NH_4HCO_3, pH 8.4, 60% acetonitrile and incubated in a thermal cycler at 100 °C for 1 h, and thereafter at 65 °C for an additional 2 h. Samples were cooled to ambient temperature, followed by addition of 100 ng of modified porcine sequencing grade trypsin (Promega) and incubated for 16 h at 37 °C. Samples were vacuum-dried and desalted using PepClean desalting columns (Pierce) according to the manufacturer's protocol. Eluted peptides were vacuum-dried and stored at −80 °C.

Human Melanoma Biopsy Sample Preparation

Cryopreserved melanoma and human skin samples were placed in a Petri dish containing phosphate-buffered saline (PBS) on wet ice and cut into small pieces with a scalpel. Tissues were transferred to microcentrifuge tubes, homogenized for 10 s, snap-frozen in liquid

nitrogen and brought to ambient temperature. Tissue lysates were sonicated for 15 sec (50 Hz) and supernatant was collected by centrifugation (2000 × *g*, 10 min). Fifty μg of each protein lysate was resolved by 1D SDS-PAGE and each lane was cut into ten equivalent slices that were digested in-gel according to established protocols.13 Briefly, gel bands were destained in 50% acetonitrile in 50 mM NH_4HCO_3, pH 8.4 and vacuum-dried. Trypsin (20 μg/mL in 25 mM NH_4HCO_3, pH 8.4) was added and samples were incubated on wet ice for 45 min. The supernatant was removed and gel bands were covered with 25 mM NH_4HCO_3, pH 8.4 and incubated at 37 °C overnight. Tryptic peptides were extracted with 70% acetonitrile, 5% formic acid, lyophilized to dryness and resuspended in 0.1% trifluoroacetic acid (TFA) prior to LC-MS/MS analysis.

Mass Spectrometry Analyses

Skin organ culture tryptic digests were analyzed in duplicate by nanoflow reversed-phase liquid chromatography (LC)-MS/MS using a nanoflow LC (Dionex Ultimate 3000, Dionex Corporation, Sunnyvale, CA) coupled online to an linear ion trap MS (LTQ-XL, ThermoFisher Scientific, San Jose, CA). Human biopsy tissue tryptic digests were similarly analyzed on an LTQ-Orbitrap MS (ThermoFisher). Separations were performed using 75 μm i.d. × 360 o.d. × 15 cm long fused silica capillary columns (Polymicro Technologies, Phoenix, AZ) slurry packed in house with 5 μm, 300 Å pore size C-18 silica-bonded stationary phase (Jupiter, Phenomenex, Torrance, CA).

Following sample injection onto a C-18 trap column (Dionex), the column was washed for 3 min with mobile phase A (2% acetonitrile, 0.1% formic acid) at a flow rate of 30 μL/min. Peptides from the SOC tissue sections were eluted using a linear gradient of 0.33% mobile phase B (0.1% formic acid in acetonitrile)/minute for 130 min, then to 95% B in an additional 15 min, all at a constant flow rate of 200 nL/min. In the case of the melanoma and skin tissue samples, peptides were eluted using a linear gradient of 1% mobile phase B/minute for 40 min, then to 95% B in an additional 10 min, all at a constant flow rate of 200 nL/min. Column washing was performed at 95% B for 15 min for all analyses, after which the column was re-equilibrated in mobile phase A prior to subsequent injections.

For the SOC analyses, the MS was operated in data-dependent MS/MS mode in which each full MS scan was followed by seven MS/MS scans performed in the linear ion trap (LIT) where the seven most abundant peptide molecular ions were selected for collision-induced dissociation (CID), using a normalized collision energy of 35%. The human melanoma and normal skin tissue digests were analyzed using a high resolution (R=60,000 at *m/z* 400) full MS scan conducted in the Orbitrap followed by tandem MS of the top five molecular ions in the LIT as described above. Data were collected over a broad precursor ion selection scan range of *m/z* 375–1800 for the SOC analysis and *m*/z 350–1800 for the analysis of the human tissue samples. Dynamic exclusion was enabled for both MS analyses to minimize redundant selection of peptides previously selected for CID.

Bioinformatic Analysis

Tandem mass spectra were searched against the UniProt human protein database (11/09 release) from the European Bioinformatics Institute (http://www.ebi.ac.uk/integr8), using SEQUEST (ThermoFisher Scientific). Additionally, peptides were searched for methionine oxidation with a mass addition of 15.9949 Da. Peptides were considered legitimately identified if they met specific charge state and proteolytic cleavage-dependent cross correlation scores of 1.9 for $[M+H]^{1+}$, 2.2 for $[M+2H]^{2+}$ and 3.5 for $[M+3H]^{3+}$, and a minimum delta correlation of 0.08. A false peptide discovery rate of approximately 2% was determined by searching the primary tandem MS data using the same criteria against a decoy database wherein the protein sequences are reversed14. Results were further filtered

using software developed in-house, and differences in protein abundance between the samples were derived by summing the total CID events that resulted in a positively identified peptide for a given protein accession across all samples (spectral counting).15 The spectral count data were normalized for each protein accession by calculating the percent contribution of the spectral count values for each protein accession against the total number of peptides identified within a given sample.16

Real-Time PCR

Total mRNA from the melanocytes and melanoma cell lines was isolated using an RNAeasy Mini Kit (Qiagen, Valencia, CA), and 1 μg of mRNA was reverse-transcribed into the corresponding first-strand cDNA with the Quantitect Transcription Kit (Qiagen). PCR reactions were performed on a MX3000P Real-Time PCR instrument (Stratagene, Agilent Technologies, Santa Clara, CA), using 1 μl of first-strand cDNA per reaction with Brilliant SYBR Green QPCR Master Mix (Stratagene). Primers (Integrated DNA Technologies, Coralville, IA) used were:

cDNA	Sequence of primers
Tenascin-C	
Forward	5’-GAGGTCAACAAAGTGGAGGCA-3’
Reverse	5’-GAGAGATTGAAGCTCTCGGGAG-3’
α-Actinin-4	
Forward	5’-CATATCAGGGGAGCGGTT-3’
Reverse	5’-GCAATAAAGTCCAGCGCT-3’
GAPDH	
Forward	5’-GAGTCAACGGATTTGGTCGT-3’
Reverse	5’-TTCATTTTGGAGGGATCTCG-3’

All experiments were performed in triplicate, fold-abundance changes in transcript levels were quantified by the ΔCt method and target gene expression was normalized to GAPDH. The VGP melanoma cell line, WM983-A, was used as a reference.

Immunoblotting and Immunostaining

Cell lysates were obtained by snap-freezing, thawing, and vortexing in lysis buffer (50 mM Hepes, pH 7.9, 0.4 M KCl, 0.5 mM EDTA, 0.1% NP-40, 10% glycerol) supplemented with 1 mM sodium orthovanadate, 50 mM sodium fluoride and protease inhibitor cocktail set V (Calbiochem, EMD Chemicals, Gibbstown, NJ). Protein concentrations were determined by the BCA assay (Pierce, Rockford, IL), and 100 μg of total protein per sample was resolved by 1D SDS-PAGE. Samples were transferred to PVDF membranes (Millipore, Billerica, MA), blocked with 5% milk in PBST and incubated with primary antibody overnight at 4 °C. Secondary antibody was added for 1 h at ambient temperature and blots were detected with SuperSignal West Pico Chemiluminescent Substrate (Pierce).

Normal human melanocytes, and likewise melanoma cells, were seeded on glass coverslips and fixed with 2% formaldehyde for 30 min at ambient temperature. After washing with PBS, cells were treated for 5 min with 0.2% Triton-X on wet ice and blocked with 5% goat serum for 30 min at ambient temperature. Incubation with anti-tenascin-C diluted in 1% goat serum was performed for 2 h at ambient temperature. After washing extensively with PBS,

secondary goat anti-mouse 488-Alexa Fluor antibody (Molecular Probes, Invitrogen) was added for 1 h. Actin fibers were stained with rhodamin phalloidin (Invitrogen) for 40 min at ambient temperature and nuclei were stained with fluorescent DAPI. Slides were mounted and images were acquired with a 60× objective using an Olympus BX-40 microscope.

Immunohistochemistry in SOCs

Paraffin-embedded specimens were cut into 5μm sections and transferred to poly-L-lysine-coated slides. Samples were deparaffinized in xylene for 2 h at 58 °C, rehydrated in a series of desending grades of alchocol and washed with de-ionized water. Antigen retrieval was performed for 15 min in 1% pepsin in 10 mM HCl for TN-C or for 20 min in citrate biffer pH 6 (Dako, Carpinteria, CA) for ACN-4. Endogenous peroxidase was blocked with 3% H_2O_2 and sections were incubated in 5% goat serum to decrease background staining. Sections were incubated with primary antibodies for 2 h in a humified 37 °C incubator, washed and incubated with biotinylated secondary goat anti-mouse antibody (Jackson ImmunoResearch, West Grove, PA) at 1:250 dilution. Immunohistochemical staining was accomplished with the Vectastatin ABC kit (PK-6100) and DAB peroxidase kit (SK-4100) (Vector Laboratories, Burlingame, CA). Slides were counterstained with Meyer's hematoxylin (Vector Laboratories), dehydrated and mounted with Permount solution (Fisher Scientific, Pittsburgh, PA). Images were acquired with a 10× objective using Olympus BX-40 microscope and SPOT imaging software (Sterling Heights, MI).

Results and Discussion

The impact of the microenvironment on the expression of proteins that govern invasion and progression of melanoma is one of the fundamental, but yet largely unresolved questions regarding this malignancy. To gain a better understanding of the underlying molecular events involved in this process, the study presented here served to determine whether an *in vivo* skin organ culture system can recapitulate protein abundance differences between melanoma cells and surrounding skin of melanoma and adjacent non-involved skin tissue samples as identified by a differential proteomic analysis. The SOCs were injected with either VGP (WM983-A) or MGP (WM1158) melanoma cell lines, or collagen alone to serve as a control. These two melanoma cell lines are widely utilized and were selected solely to compare melanoma growth to normal (e.g. non-invovled) skin in this SOC model and not to provide a detailed comparison of VGP versus MGP. Approximately 10,000 cells were collected by laser microdissection from these FFPE SOC sections (Fig. 2A). The microdissected cells were processed using an "MS-friendly" heat-induced, enzyme-mediated (HI/EM) antigen retrieval method, followed by trypsin digestion (Fig. 2B). Peptide digests were analyzed by LC-MS/MS; Figure 2C shows a representative basepeak chromatogram of a digest from approximately 5,000 cells on column from the microdissected FFPE VGP melanoma SOC section. This analysis afforded the identification of upwards of several hundred proteins per sample at a false discovery rate of approximately 2%, with all samples processed in duplicate.

Differences in protein abundance between the various SOC-derived samples were derived by spectral counting, where it was found that proteins such as tenascin-C (TN-C) and fibronectin, which have been described in the literature to play a role in melanoma cell invasion17, 18, were identified by high spectral count in the MGP melanoma SOC sections, and at lower levels in the VGP melanoma SOC sections (Table 1). These proteins were either not identified or were identified at very low abundance in the the collagen and non-injected SOC controls. Increases in the abundance of TN-C have been documented in MGP melanomas, and it has been suggested that relatively low levels of TN-C expression may be associated with a lower risk for metastasis19. Like TN-C, fibronectin is another protein implicated in melanoma invasion. Specifically, it has been reported that these two proteins

stimulate the invasive features of primary melanoma cells in 3-D collagen matrices, and that TN-C, fibronectin and procollagen I form specific channel structures for melanoma invasion18. Tenascin-C and fibronectin are produced not only by fibroblasts, but also by endothelial cells and keratinocytes20. However, it is not yet fully established to what extent these proteins are also produced by VGP and/or MGP melanoma cells. The data presented here document that melanocytes, propagated *in vitro*, do not produce detectable levels of TN-C (Fig. 3) and only low levels of fibronectin (data not shown). In contrast, both MGP and VGP melanoma cells express substantial amounts of these matrix proteins. These matrix components are not only secreted but also incorporated into an insoluble matrix surrounding the cells, likely giving rise to the apparent difference in the relative levels of TN-C transcript versus protein abundances measured in this study. The important point regarding this finding is that these melanoma cells produce these matrix components which are known to drive cell migration and tumor invasion21.

α-Actinin-4 (ACN4) is another protein identified as differentially abundant between the SOC melanoma samples and controls. Furthermore, as depicted in Figure 4, this protein is clearly present at higher levels in melanoma cells compared to melanocytes, both at the level of the transcript and protein. α-Actinin-4 is an actin cytoskeleton filament bundling protein and plays crucial roles in cell migration and cytokinesis22. In addition, growth factor signaling is important for dynamic control of ACN4/actin filament interactions, which in turn regulates cell adhesion during substratum attachment and nuclear segregation during mitosis23.

The increased expression of both TN-C and ACN4 was verified by immunohistochemistry (IHC) in WM983-A injected SOCs in the region of the tumor lesion as compared to the collagen-injected controls (Fig. 5). As expected, TN-C appears to be localized to the extracellular space (Fig. 5A) whereas ACN4 expression is primarily observed to be intracellular (Fig. 5C). While low levels of TN-C can be observed in the collagen-injected SOC, this observation likely arises from the fact that these skin cultures are immature and composed of neonatal fibroblasts and kerationcytes, both of which produce TN-C.

Thrombospondin-1 (TSP-1) was identified with an elevated abundance in both the MGP and VGP SOC sections compared to the controls. TSP-1 is a secreted protein that plays a role in tissue remodeling, is upregulated in response to injury and inflammation24 and has been detected at elevated levels in sera of patients with advanced melanoma25–27. Plectin was also substantially more abundant in the MGP melanoma cells than in the VGP melanoma cells. Plectin, a structural protein found in nearly every cell type, interacts with numerous cytoskelatal components and has a role in the interactions of intracellular junctions and contributes to tissue integrity28, 29. Plectin has been shown to be upregulated in pancreatic and colon cancer30, 31, but there are no reports that cite this protein as being expressed in advanced melanomas. Similar to tenascin-C and fibronectin, plectin was identified with an increased relative abundance in the melanoma tissue sample as compared to that of the normal skin sample.

Alpha-enolase and pyruvate kinase M2 were identified with elevated abundances in the MGP SOC section relative to the other SOC samples. Increased levels of α-enolase have been previously associated with tumor cell migration and metastasis32 and has been shown to be elevated in several metastatic melanoma cell lines33, 34. This increased expression level of α-enolase and pyruvate kinase M2 may reflect the apparent increased utilization of glycolysis for ATP generation in tumor cells as suggested by Warburg35.

There are a number of notable proteins identified in the present study that merit further investigation. Of these, transgelin 2, a homolog of transgelin and member of a family of

actin-binding proteins that is proposed to be involved in cytoskeletal cross-linking and polymerization, was identified in greater relative abundance in the MGP SOC tissue section as compared to the other samples. There are several reports citing an upregulation of transgelins in gastric36 and colorectal37 cancers. Transgelin has been shown to be involved with ERK-related signal transduction, however, the function of transgelin in cancer development and progression remains to be elucidated. The cytokeratin (CK) pairs 5/14 and 6/16 and 17 were observed with decreased abundances in the VGP SOC section. It is well known that cytokeratins play a significant role in the organization and integrity of cellular structure and are indicators for differentiation state and metastatic nature of tumor cells. A previous study established diminished expression levels of CK 5/14 and 6/16 and 17 in metastatic melanoma38. The present analyses also reveal an apparent increase in the abundance of pulmonary surfactant protein D in the VGP SOC section. While its role in melanoma has not been fully explored, the gene encoding this protein has been shown to be induced in a variety of metastatic pulmonary and non-small cell lung cancers, and is detectable in a variety of others, such as gastric, pancreas and prostate39.

Conclusions

The findings of these proteomic analyses establish the feasibility of using SOCs for evaluating the tumor microenvironment and the changes in the molecular events that drive invasion and progression of melanoma. Melanoma cell lines, representing VGP and MGP melanoma, injected into SOCs demonstrate the ability to perform a differential proteomic analysis using a spectral count approach and generation of proteomic profiles which very closely resemble those obtained from an analysis of differential protein abundances from melanoma and normal skin biopsy tissues. Indeed, several known melanoma-related proteins, such as tenascin-C and fibronectin, were identified at different relative abundances in the SOCs which directly correspond to the abundance differences observed in the analysis of the tissue biopsy samples. These data suggest that melanoma-seeded SOCs represent a unique model system to gain further insight regarding proteins that support melanoma cell invasion and the crosstalk between melanoma cells and the skin microenvironment.

Supplementary Material

Refer to Web version on PubMed Central for supplementary material.

Acknowledgments

This work was supported by the David Scaife Foundation (TPC), in-kind contributions from the Pittsburgh VA HealthCare System (AW) and a grant from the National Institutes of Health (DB). The authors would like to thank Dr Zhou Wang for the use of the laser microscope, Diane George for technical assistance and the helpful advice from the two anonymous reviewers.

References

1. Baruthio F, Quadroni M, Ruegg C, Mariotti A. Proteomic analysis of membrane rafts of melanoma cells identifies protein patterns characteristic of the tumor progression stage. Proteomics. 2008; 8(22):4733–4747. [PubMed: 18942674]
2. Paulitschke V, Kunstfeld R, Mohr T, Slany A, Micksche M, Drach J, Zielinski C, Pehamberger H, Gerner C. Entering a new era of rational biomarker discovery for early detection of melanoma metastases: secretome analysis of associated stroma cells. J Proteome Res. 2009; 8(5):2501–2510. [PubMed: 19222175]
3. Forgber M, Trefzer U, Sterry W, Walden P. Proteome serological determination of tumor-associated antigens in melanoma. PLoS One. 2009; 4(4):e5199. [PubMed: 19381273]

4. Caron J, Mange A, Guillot B, Solassol J. Highly sensitive detection of melanoma based on serum proteomic profiling. J Cancer Res Clin Oncol. 2009; 135(9):1257–1264. [PubMed: 19288131]
5. Hu M, Polyak K. Molecular characterisation of the tumour microenvironment in breast cancer. Eur J Cancer. 2008; 44(18):2760–2765. [PubMed: 19026532]
6. Meier F, Nesbit M, Hsu MY, Martin B, Van Belle P, Elder DE, Schaumburg-Lever G, Garbe C, Walz TM, Donatien P, Crombleholme TM, Herlyn M. Human melanoma progression in skin reconstructs : biological significance of bFGF. Am. J. Pathol. 2000; 156(1):193–200. [PubMed: 10623667]
7. Neil SM, Eves P, Richardson B, Molife R, Lorigan P, Wagner M, Layton C, Morandini R, Ghanem G. Oestrogenic steroids and melanoma cell interaction with adjacent skin cells influence invasion of melanoma cells in vitro. Pigment Cell Res. 2000; 13(Suppl 8):68–72. [PubMed: 11041360]
8. Eves P, Layton C, Hedley S, Dawson RA, Wagner M, Morandini R, Ghanem G, Mac Neil S. Characterization of an in vitro model of human melanoma invasion based on reconstructed human skin. Br J Dermatol. 2000; 142(2):210–222. [PubMed: 10730751]
9. Eves P, Katerinaki E, Simpson C, Layton C, Dawson R, Evans G, Mac Neil S. Melanoma invasion in reconstructed human skin is influenced by skin cells--investigation of the role of proteolytic enzymes. Clin Exp Metastasis. 2003; 20(8):685–700. [PubMed: 14713103]
10. Herlyn M, Ferrone S, Ronai Z, Finerty J, Pelroy R, Mohla S. Melanoma biology and progression. Cancer Res. 2001; 61(11):4642–4643. [PubMed: 11389102]
11. Margulis A, Zhang W, Garlick JA. In vitro fabrication of engineered human skin. Methods Mol Biol. 2005; 289:61–70. [PubMed: 15502170]
12. Becker JK, Goldberg LH, Tschen JA. Differential diagnosis of malignant melanoma. Am Fam Physician. 1989; 39(5):203–214. [PubMed: 2655407]
13. Wilm M, Shevchenko A, Houthaeve T, Breit S, Schweigerer L, Fotsis T, Mann M. Femtomole sequencing of proteins from polyacrylamide gels by nano-electrospray mass spectrometry. Nature. 1996; 379(6564):466–469. [PubMed: 8559255]
14. Elias JE, Gygi SP. Target-decoy search strategy for increased confidence in large-scale protein identifications by mass spectrometry. Nat Methods. 2007; 4(3):207–214. [PubMed: 17327847]
15. Liu H, Sadygov RG, Yates JR 3rd. A model for random sampling and estimation of relative protein abundance in shotgun proteomics. Anal. Chem. 2004; 76(14):4193–4201. [PubMed: 15253663]
16. Patel V, Hood BL, Molinolo AA, Lee NH, Conrads TP, Braisted JC, Krizman DB, Veenstra TD, Gutkind JS. Proteomic analysis of laser-captured paraffin-embedded tissues: a molecular portrait of head and neck cancer progression. Clin Cancer Res. 2008; 14(4):1002–1014. [PubMed: 18281532]
17. Fukunaga-Kalabis M, Santiago-Walker A, Herlyn M. Matricellular proteins produced by melanocytes and melanomas: in search for functions. Cancer Microenviron. 2008; 1(1):93–102. [PubMed: 19308688]
18. Kaariainen E, Nummela P, Soikkeli J, Yin M, Lukk M, Jahkola T, Virolainen S, Ora A, Ukkonen E, Saksela O, Holtta E. Switch to an invasive growth phase in melanoma is associated with tenascin-C, fibronectin, and procollagen-I forming specific channel structures for invasion. J Pathol. 2006; 210(2):181–191. [PubMed: 16924594]
19. Ilmonen S, Jahkola T, Turunen JP, Muhonen T, Asko-Seljavaara S. Tenascin-C in primary malignant melanoma of the skin. Histopathology. 2004; 45(4):405–411. [PubMed: 15469480]
20. Jones FS, Jones PL. The tenascin family of ECM glycoproteins: structure, function, and regulation during embryonic development and tissue remodeling. Dev Dyn. 2000; 218(2):235–259. [PubMed: 10842355]
21. Iyer AKV, Tran KT, Griffith L, Wells A. Cell surface restriction of EGFR by a Tenascin cytotactin-encoded EGF-like repeat is preferential for motility-related signaling. J. Cell. Physiol. 2007; 214:504–512. [PubMed: 17708541]
22. Sjoblom B, Salmazo A, Djinovic-Carugo K. Alpha-actinin structure and regulation. Cell Mol Life Sci. 2008; 65(17):2688–2701. [PubMed: 18488141]
23. Shao H, Wu C, Wells A. Phosphorylation of alpha-actinin-4 upon epidermal growth factor (EGF) exposure regulates its interaction with actin. J. Biol. Chem. 2009

24. Bornstein P. Thrombospondins as matricellular modulators of cell function. J. Clin. Invest. 2001; 107(8):929–934. [PubMed: 11306593]
25. Sid B, Sartelet H, Bellon G, El Btaouri H, Rath G, Delorme N, Haye B, Martiny L. Thrombospondin 1: a multifunctional protein implicated in the regulation of tumor growth. Crit Rev Oncol Hematol. 2004; 49(3):245–258. [PubMed: 15036264]
26. Bornstein P. Thrombospondins function as regulators of angiogenesis. J Cell Commun Signal. 2009
27. Rofstad EK, Graff BA. Thrombospondin-1-mediated metastasis suppression by the primary tumor in human melanoma xenografts. J. Invest. Dermatol. 2001; 117(5):1042–1049. [PubMed: 11710911]
28. Svitkina TM, Verkhovsky AB, Borisy GG. Plectin sidearms mediate interaction of intermediate filaments with microtubules and other components of the cytoskeleton. J. Cell Biol. 1996; 135(4): 991–1007. [PubMed: 8922382]
29. Wiche G. Plectin: general overview and appraisal of its potential role as a subunit protein of the cytomatrix. Crit. Rev. Biochem. Mol. Biol. 1989; 24(1):41–67. [PubMed: 2667895]
30. Bausch D, Mino-Kenudson M, Fernandez-Del Castillo C, Warshaw AL, Kelly KA, Thayer SP. Plectin-1 is a Biomarker of Malignant Pancreatic Intraductal Papillary Mucinous Neoplasms. J Gastrointest Surg. 2009
31. Lee KY, Liu YH, Ho CC, Pei RJ, Yeh KT, Cheng CC, Lai YS. An early evaluation of malignant tendency with plectin expression in human colorectal adenoma and adenocarcinoma. J Med. 2004; 35(1–6):141–149. [PubMed: 18084872]
32. Liu K, Shih N. The Role of Enolase in Tissue Invasion and Metastasis of Pathogens and Tumor Cells. Journal of Cancer Molecules. 2007; 3:45–48.
33. Nawarak J, Huang-Liu R, Kao SH, Liao HH, Sinchaikul S, Chen ST, Cheng SL. Proteomics analysis of A375 human malignant melanoma cells in response to arbutin treatment. Biochim. Biophys. Acta. 2009; 1794(2):159–167. [PubMed: 18996230]
34. Rodeck U, Melber K, Kath R, Menssen HD, Varello M, Atkinson B, Herlyn M. Constitutive expression of multiple growth factor genes by melanoma cells but not normal melanocytes. J. Invest. Dermatol. 1991; 97(1):20–26. [PubMed: 2056188]
35. Warburg O, Geissler AW, Lorenz S. Genesis of tumor metabolism by vitamin B1 deficiency (thiamine deficiency). Z Naturforsch B. 1970; 25(3):332–333. [PubMed: 4392802]
36. Huang Q, Chen W, Wang L, Lin W, Lin J, Lin X. Identification of transgelin as a potential novel biomarker for gastric adenocarcinoma based on proteomics technology. J Cancer Res Clin Oncol. 2008; 134(11):1219–1227. [PubMed: 18446369]
37. Zhang Y, Ye Y, Shen D, Jiang K, Zhang H, Sun W, Zhang J, Xu F, Cui Z, Wang S. Identification of transgelin-2 as a biomarker of colorectal cancer by laser capture microdissection and quantitative proteome analysis. Cancer Sci. 2009
38. Riker AI, Enkemann SA, Fodstad O, Liu S, Ren S, Morris C, Xi Y, Howell P, Metge B, Samant RS, Shevde LA, Li W, Eschrich S, Daud A, Ju J, Matta J. The gene expression profiles of primary and metastatic melanoma yields a transition point of tumor progression and metastasis. BMC Med Genomics. 2008; 1:13. [PubMed: 18442402]
39. Betz C, Papadopoulos T, Buchwald J, Dammrich J, Muller-Hermelink HK. Surfactant protein gene expression in metastatic and micrometastatic pulmonary adenocarcinomas and other non-small cell lung carcinomas: detection by reverse transcriptase-polymerase chain reaction. Cancer Res. 1995; 55(19):4283–4286. [PubMed: 7671236]

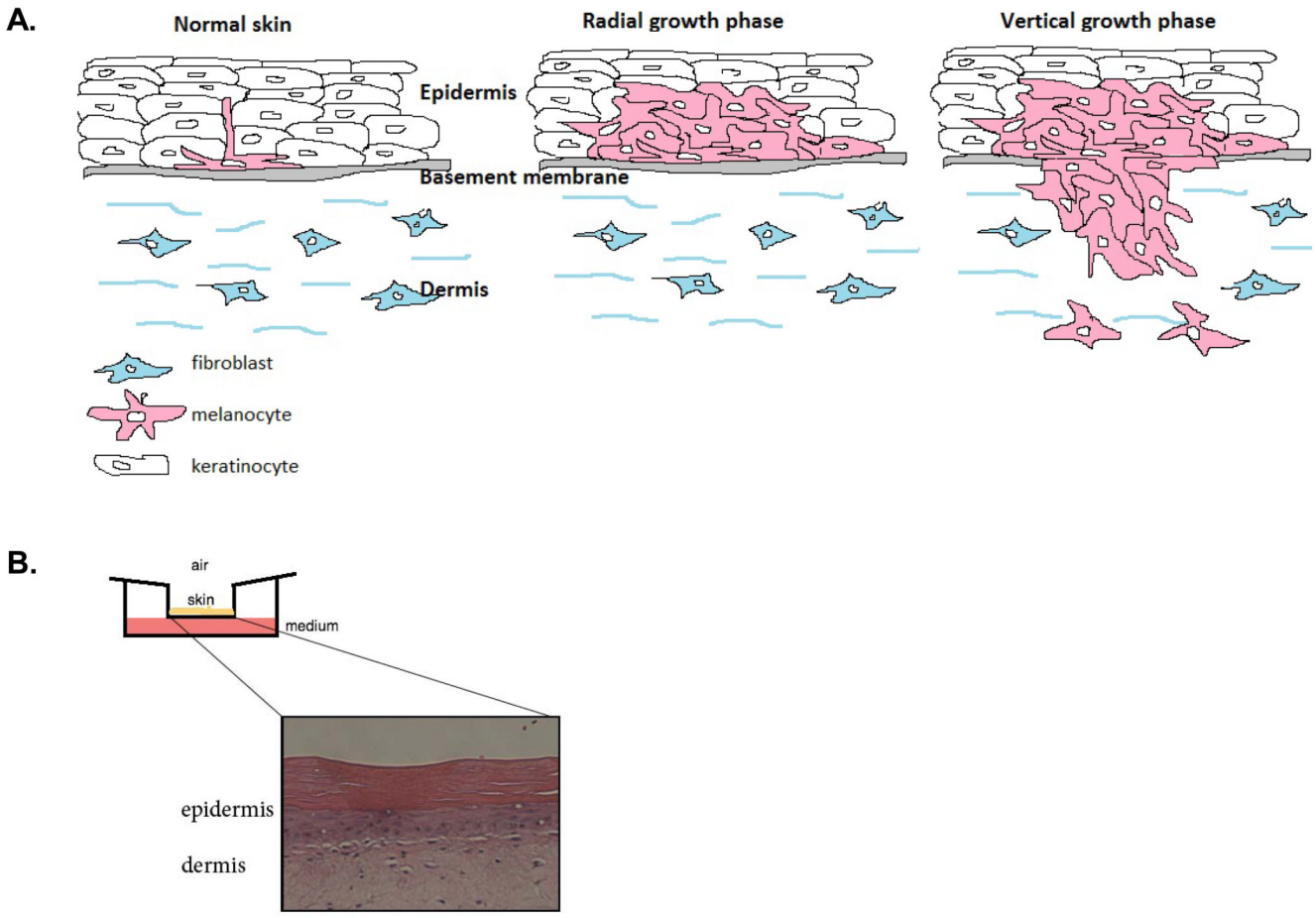

Figure 1.

A. Cartoon depicting stages of melanoma progression in skin. Melanocytes reside in the epidermal/dermal junction. Early-stage radial growth phase melanoma cells descend into the papillary dermis and spread laterally. Invasion deep into the dermis characterizes melanomas in the vertical groth phase. **B. Cartoon of a skin organ culture (SOC)**. SOCs are maintained at the air-liquid interface. The inset depicts a hematoxylin & eosin stained section collected on day 12 of culture.

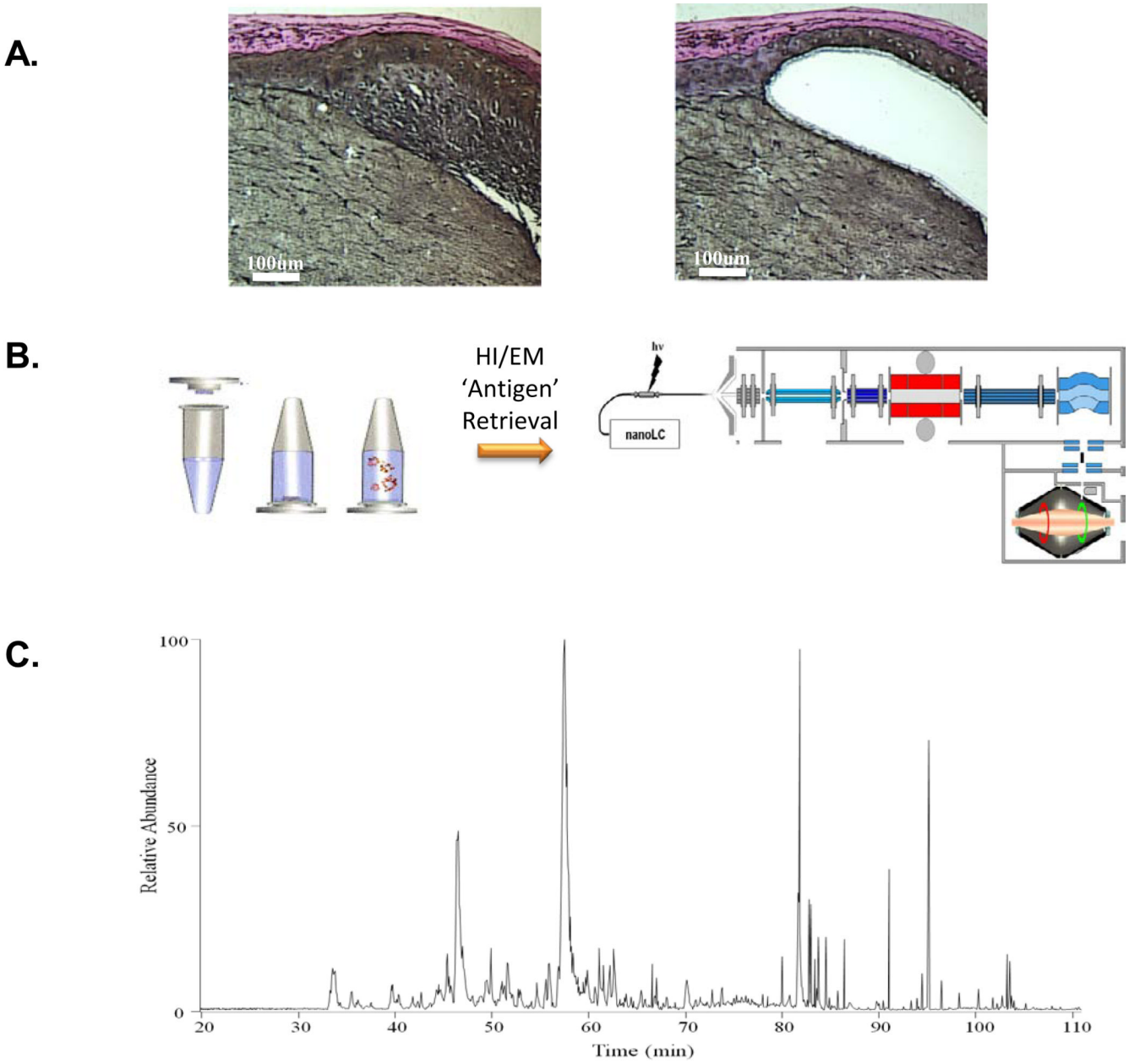

Figure 2. Mass spectrometry-based proteomic analysis of melanoma and skin organ cultures

A. Hematoxylin & eosin staining of formalin-fixed, paraffin-embedded (FFPE) skin organ culture (SOC) sections injected with approximately 10,000 VGP melanoma cells (WM983-A) before (left panel) and after (right panel) laser microdissection. C. Basepeak chromatogram of approximately 5,000 VGP melanoma cells obtained by laser microdissection from the FFPE SOC tissue sections.

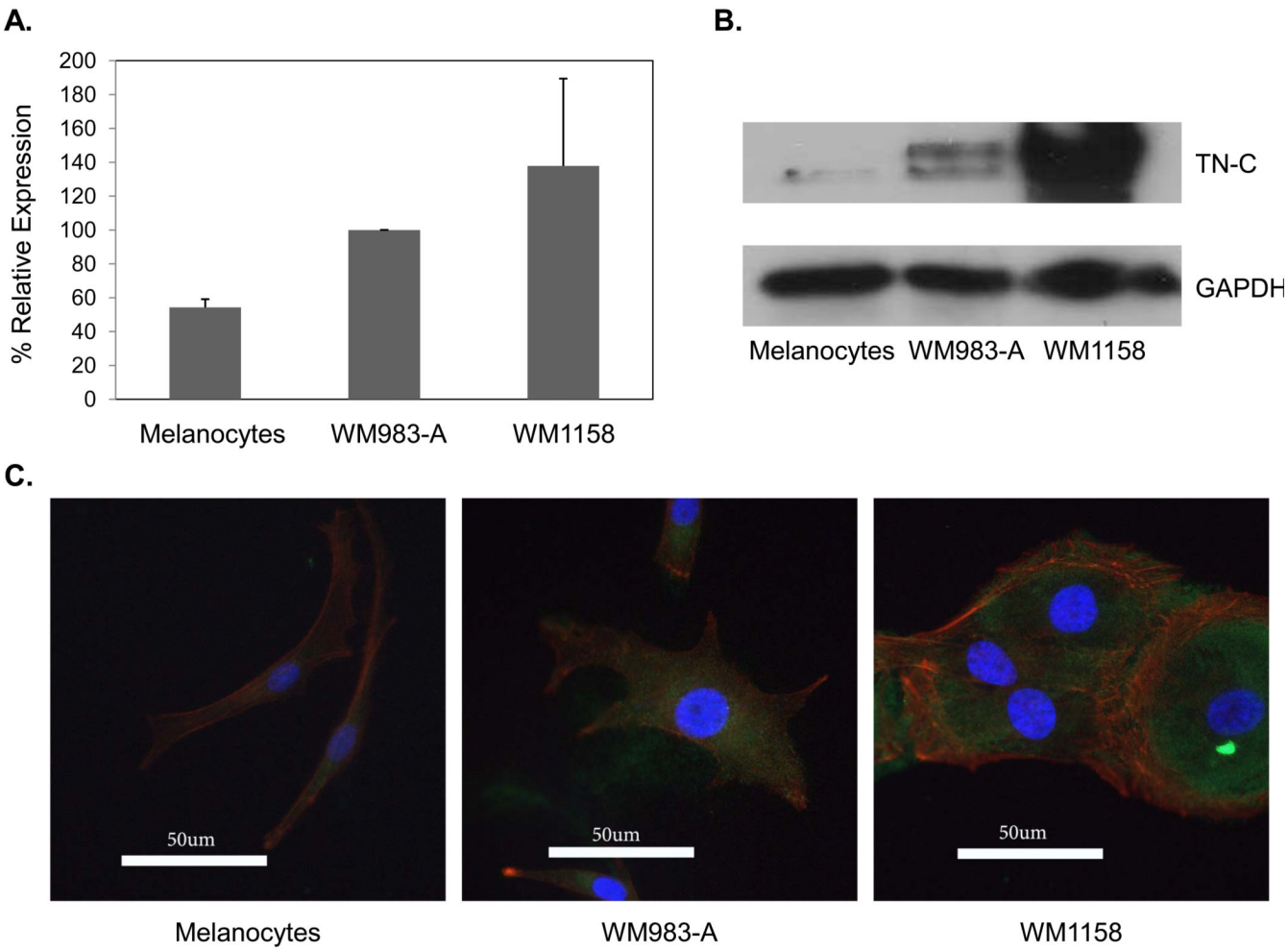

Figure 3. Expression of tenascin-C in melanoma cells

A. Quantitative RT-PCR analysis of the expression of tenascin-C (TN-C) mRNA in WM983-A (VGP) and WM1158 (MGP) melanoma cells compared to human melanocytes, propagated *in vitro*. The data are expressed as the mean±standard deviation from three independent experiments. B. Immunoblot analysis depicting the level of TN-C in the VGP and MGP melanoma cell lines and melanocytes. C. Immunofluorescence analysis of melanocytes and VGP and MGP melanoma cell lines, probed with antibody to TN-C (pseudocolored green) and actin (pseudocolored red). The cells were counterstained with fluorescent DAPI (pseudocolored blue).

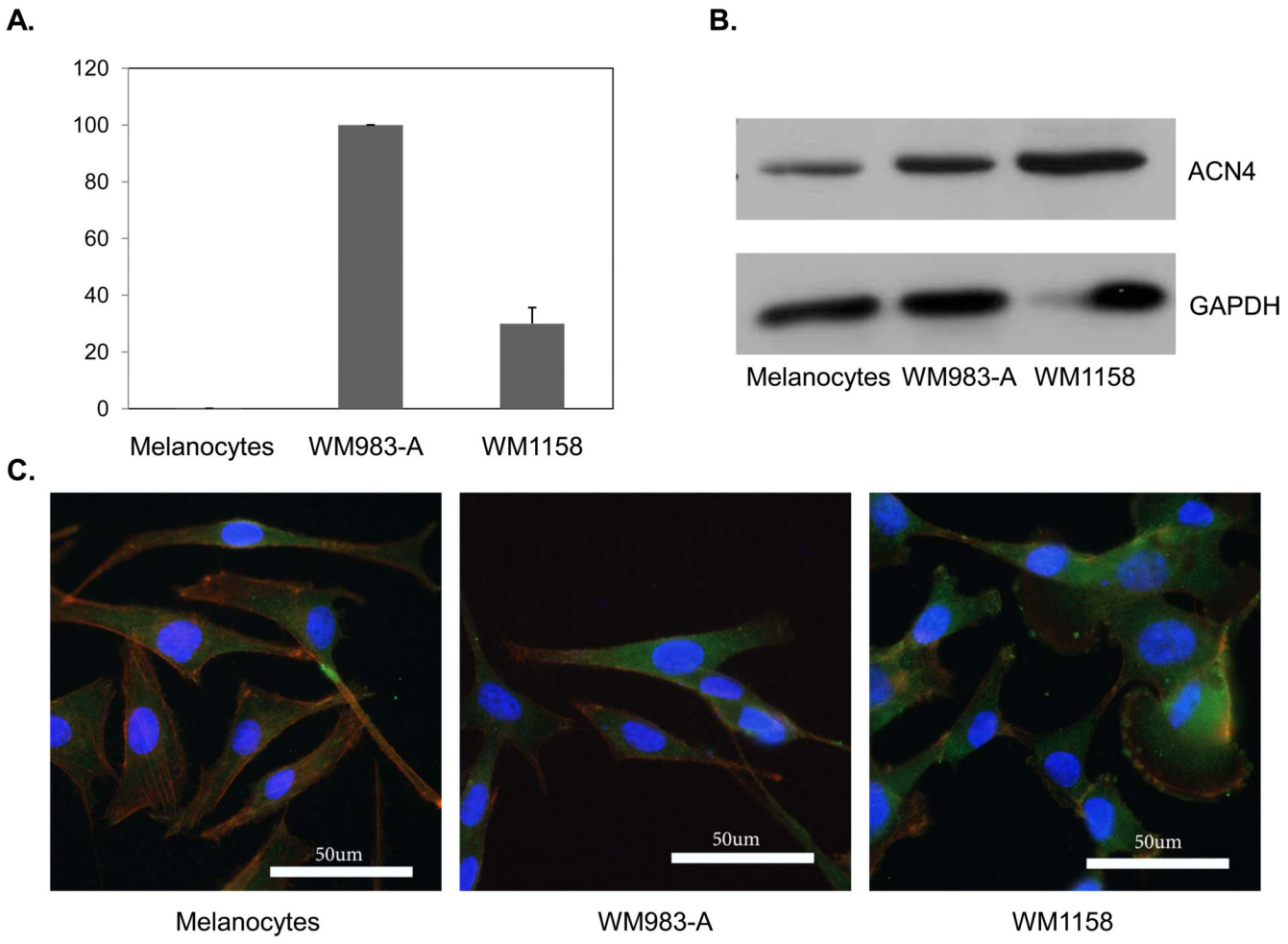

Figure 4. Alpha-actinin-4 expression melanoma cells

A. Quantitative RT-PCR analysis of α-actinin-4 (ACN4) expression in the WM983-A (VGP) and WM1158 (MGP) melanoma cell lines and in melanocytes. The data are expressed as the mean ±standard deviation from three independent experiments. B. Immunoblot analysis of ACN4 expression in the VGP and MGP melanoma cell lines and in melanocytes. C. Immunofluorescence analysis of melanocytes and VGP and MGP melanoma cell lines, probed with antibody to ACN4 (pseudocolored green) and actin (pseudocolored red). The cells were counterstained with fluorescent DAPI (pseudocolored blue).

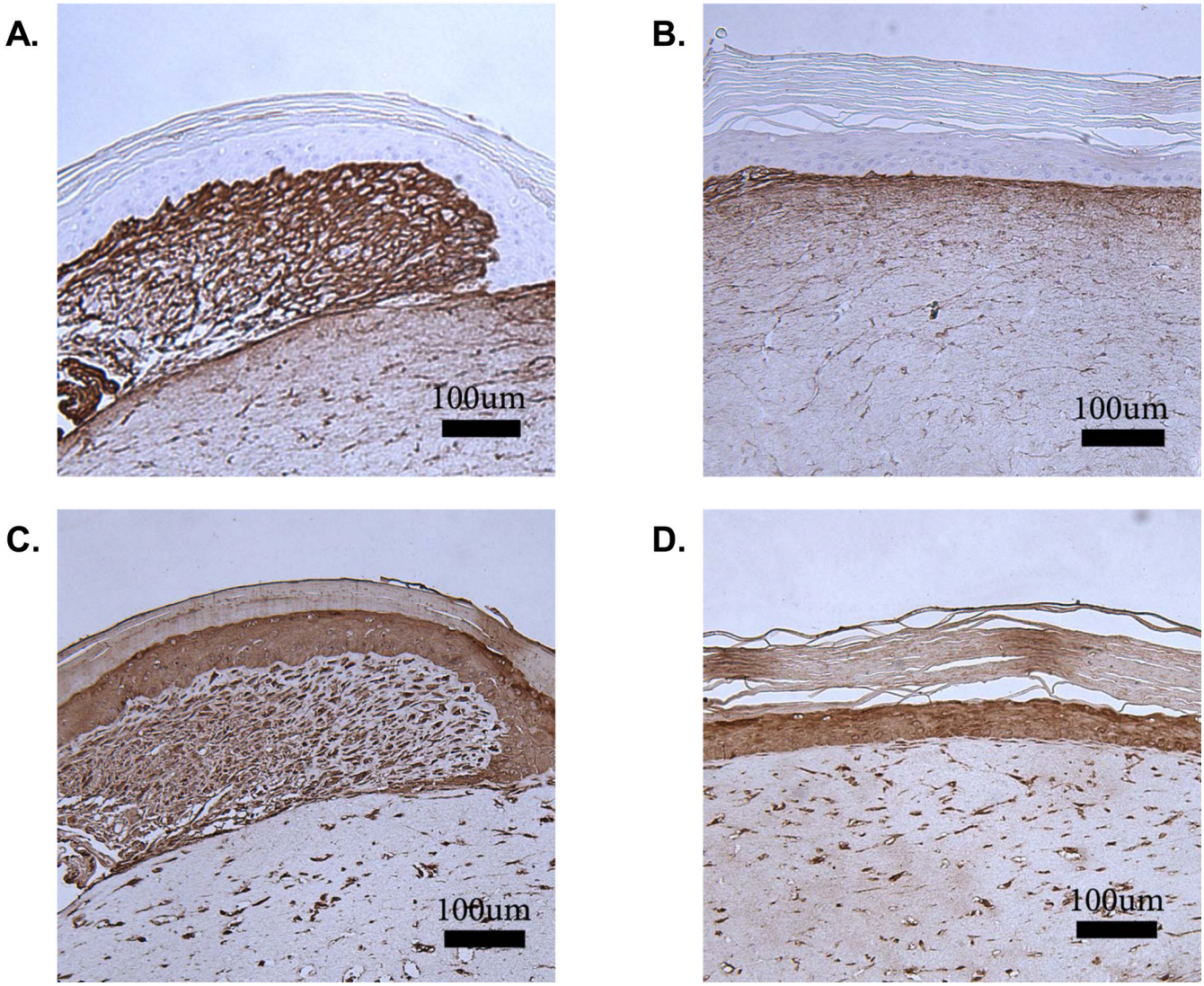

Figure 5. Immunohistochemical analysis of tenascin-C and α-actinin-4 in SOCs

Immunohistochemical analysis of the expression of tenascin-C (TN-C) (A) and α-actinin-4 (ACN4) (C) in SOCs injected with WM983-A melanoma cells compared to collagen injection controls (B and D).

J Proteome Res. Author manuscript; available in PMC 2013 August 05.

Table 1

Spectral count data for selected extracellular matrix and cytoskeletal proteins identified in melanoma-injected or control SOCs and from melanoma and normal human skin tissue.

Protein	Function	SOC WM1158*	SOC WM983-A	SOC Collagen	SOC Ctrl	Biopsy Melanoma	Biopsy Normal
Tenascin-C	Matrix	19	7	1	0	143	0
Fibronectin	Adhesion/Cytoskeleton	11	6	0	0	46	20
Collagen 1	Matrix	17	8	6	10	15	107
α–Actinin-4	Adhesion/Cytoskeleton	2	1	0	0	76	22
Thrombospondin-1	Adhesion/Matrix	2	2	0	0	4	1
Plectin	Adhesion/Cytoskeleton	17	1	0	1	153	15
Transgelin 2	Adhesion/Cytoskeleton	6	0	0	0	14	18
Cytokeratin 5	Adhesion/Cytoskeleton	69	9	30	31	43	9
Cytokeratin 14	Adhesion/Cytoskeleton	56	1	22	13	25	14
Cytokeratin 6A	Adhesion/Cytoskeleton	41	6	26	30	17	0
Cytokeratin 16	Adhesion/Cytoskeleton	17	0	7	5	11	0
Cytokeratin 17	Adhesion/Cytoskeleton	22	0	5	4	1	0

*WM1158 - MGP melanoma cells injected into SOC

WM983-A - VGP melanoma cells injected into SOC

Coll - collagen injection into SOC

Ctrl – no injection SOC